

Charge Transfer in the Electron Donor–Acceptor Complex BH₃NH₃

Yirong Mo,^{*,†,‡} Lingchun Song,[‡] Wei Wu,^{*,‡} and Qianer Zhang[‡]

Contribution from the Department of Chemistry, Western Michigan University, Kalamazoo, Michigan 49008, and Department of Chemistry, the State Key Laboratory for Physical Chemistry of Solid States, Center for Theoretical Chemistry, Xiamen University, Xiamen, Fujian 361005, P. R. China

Received November 24, 2003; E-mail: yirong.mo@wmich.edu; weiwu@xmu.edu.cn

Abstract: As a simple yet strongly binding electron donor–acceptor (EDA) complex, BH₃NH₃ serves as a good example to study the electron pair donor–acceptor complexes. We employed both the ab initio valence bond (VB) and block-localized wave function (BLW) methods to explore the electron transfer from NH₃ to BH₃. Conventionally, EDA complexes have been described by two diabatic states: one neutral state and one ionic charge-transferred state. Ab initio VB self-consistent field (VBSCF) computations generate the energy profiles of the two diabatic states together with the adiabatic (ground) state. Our calculations evidently demonstrated that the electron transfer between NH₃ and BH₃ falls in the abnormal regime where the reorganization energy is less than the exoergicity of the reaction. The nature of the NH₃–BH₃ interaction is probed by an energy decomposition scheme based on the BLW method. We found that the variation of the charge-transfer energy with the donor–acceptor distance is insensitive to the computation levels and basis sets, but the estimation of the amount of electron transferred heavily depends on the population analysis procedures. The recent resurgence of interest in the nature of the rotation barrier in ethane prompted us to analyze the conformational change of BH₃NH₃, which is an isoelectronic system with ethane. We found that the preference of the staggered structure over the eclipsed structure of BH₃NH₃ is dominated by the Pauli exchange repulsion.

Introduction

Electron donor–acceptor (EDA) complexes, which are bound together by the dative bond and also called partially bonded molecules, have been the subjects of active research due to their peculiar chemical and physical properties.¹ The bond strength in EDA complexes is about the average of strong covalent bond and weak van der Waals bond. Usually EDA complexes are brightly colored or semiconductors in the solid state, and these physical properties are related to the electron-transfer nature from the donor to the acceptor. A typical class of EDA complexes involves electron-deficient boranes as Lewis acids and electron-rich amines as Lewis bases. As a matter of fact, the boron–nitrogen dative bond, which is the classical example to demonstrate the electron transfer from the lone nitrogen pair to the vacant orbital on boron, has important physiological activities.² The simplest system in this category is BH₃NH₃, which has been extensively studied experimentally^{3–5} and computationally.^{6–10} Most recently, Horváth et al. analyzed the

variations of geometrical and electronic characteristics along the donor–acceptor distance in a few donor–acceptor complexes, including BH₃NH₃ at the MP2(fc)/6-311+G(2df,p) level.¹¹

In general, Pearson's hard and soft acid base (HSAB) principle provides a qualitative guideline to understand the relative stabilities of donor–acceptor adducts,¹² and Mulliken

[†] Western Michigan University.

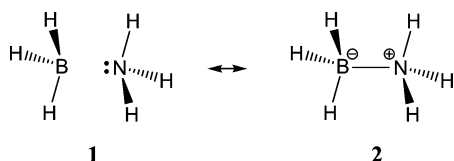
[‡] Xiamen University.

- (1) Leopold, K. R.; Canagaratna, M.; Phillips, J. A. *Acc. Chem. Res.* **1997**, *30*, 57–64.
- (2) Fisher, L. S.; McNeil, K.; Butzen, J.; Holme, T. A. *J. Phys. Chem. B* **2000**, *104*, 3744–3751.
- (3) Thorne, L. R.; Suenram, R. D.; Lovas, F. J. *J. Chem. Phys.* **1983**, *78*, 167–171.
- (4) Klooster, W. T.; Koetzle, T. F.; Siegbahn, P. E. M.; Richardson, T. B.; Crabtree, R. H. *J. Am. Chem. Soc.* **1999**, *121*, 6337–6343.
- (5) Trudel, S.; Gilson, D. F. R. *Inorg. Chem.* **2003**, *42*, 2814–2816.

- (6) (a) Peyerimhoff, S. D.; Buenker, R. J. *J. Chem. Phys.* **1968**, *49*, 312. (b) Dill, J. D.; Schleyer, P. v. R.; Pople, J. A. *J. Am. Chem. Soc.* **1975**, *97*, 3402–3409. (c) Eoeggen, I. *Chem. Phys.* **1992**, *162*, 271–284. (d) Umeyama, H.; Morokuma, K. *J. Am. Chem. Soc.* **1976**, *98*, 7208–7220. (e) Holme, T. A.; Truong, T. N. *Chem. Phys. Lett.* **1993**, *215*, 53–57. (f) Sakai, S. *J. Phys. Chem.* **1995**, *99*, 9080–9086. (g) Glendening, E. D.; Streitwieser, A. *J. Chem. Phys.* **1994**, *100*, 2900–2909. (h) Dapprich, S.; Frenking, G. *J. Phys. Chem.* **1995**, *99*, 9352–9362. (i) Skancke, A.; Skancke, P. N. *J. Phys. Chem.* **1996**, *100*, 15079–15082.
- (7) Jonas, V.; Frenking, G.; Reetz, M. T. *J. Am. Chem. Soc.* **1994**, *116*, 8741–8753.
- (8) (a) Branchadell, V.; Sbai, A.; Oliva, A. *J. Phys. Chem.* **1995**, *99*, 6472–6476. (b) Allendorf, M. D.; Melius, C. F. *J. Phys. Chem. A* **1997**, *101*, 2670–2680. (c) Bauschlicher, C. W. J.; Ricca, A. *Chem. Phys. Lett.* **1995**, *237*, 14–19. (d) Anane, H.; Boutalib, A.; Tomas, F. *J. Phys. Chem. A* **1997**, *101*, 7879–7884. (e) Anane, H.; Boutalib, A.; Nebot-Gil, I.; Tomas, F. *J. Phys. Chem. A* **1998**, *102*, 7070–7073. (f) Es-Sofi, A.; Serrac, C.; Ouassas, A.; Jarid, A.; Boutalib, A.; Nebot-Gil, I.; Tomas, F. *J. Phys. Chem. A* **2002**, *106*, 9065–9070. (g) Barrios, R.; Skurski, P.; Rak, J.; Gutowski, M. *J. Chem. Phys.* **2000**, *113*, 8961–8968. (h) Dillen, J.; Verhoeven, P. *J. Phys. Chem. A* **2003**, *107*, 2570–2577.
- (9) Timoshkin, A. Y.; Suvorov, A. V.; Bettinger, H. F.; Schaefer, H. F., III. *J. Am. Chem. Soc.* **1999**, *121*, 5687–5699.
- (10) Mo, Y.; Gao, J. *J. Phys. Chem. A* **2001**, *105*, 6530–6536.
- (11) Horváth, V.; Kovacs, A.; Hargittai, I. *J. Phys. Chem. A* **2003**, *107*, 1197–1202.
- (12) (a) Pearson, R. G. *J. Am. Chem. Soc.* **1963**, *85*, 3533–3539. (b) Pearson, R. G. *Chemical Hardness: Applications from Molecules to Solids*; Wiley-VCH: Weinheim, Germany, 1997.

proposed that an acid–base adduct is formed by the charge transfer from the HOMO of the base and the LUMO of the acid in the framework of molecular orbital (MO) theory.¹³ The intriguing issues in the donor–acceptor adducts are how to probe the magnitude of electron transfer from a donor to an acceptor and whether this magnitude in one way or another is related to the bond strength, geometrical variation, and physiochemical properties. Although earlier works indeed showed the linear correlation between the degree of charge transfer and the dissociation energy,¹⁴ recent works suggested otherwise.^{7,9} From the experimental perspectives, nuclear quadrupole coupling constants^{15,16} and vibrational frequencies¹⁷ have been found to be correlated to the charge-transfer effect.

In terms of resonance theory, BH_3NH_3 can be well described by the following two resonance structures (or diabatic states):



For the first structure where no bond exists between the two moieties, the nitrogen lone pair completely retains in the amine moiety, and the interaction between BH_3 and NH_3 does not involve the electron-transfer effect and thus falls in the category of the van der Waals physical interaction. For the second structure, however, the nitrogen lone pair in NH_3 is now equally shared by the acceptor BH_3 and forms a typical covalent (dative) bond. According to the Pauling–Wheland rules,^{18,19} the neutral resonance structure **1** should be more stable than the ionic structure **2**. Consequently, the ground state for the complex is a linear combination of the no-bond and dative structures, with less importance of the latter ionic structure.

BH_3NH_3 is isoelectronic with ethane, but the bond strength (31.1 kcal/mol) is only one-third of the latter.²⁰ The contribution from the ionic resonance structure is highlighted by the high dipole moment (5.216 D),³ suggesting that there is a significant charge transfer from NH_3 to BH_3 . The consequence of the intermolecular electron transfer is that the hydrogen atoms in the NH_3 moiety carry a fraction of positive charge, whereas those in the BH_3 moiety carry negative charges. The interaction between hydride atoms and protons forms unconventional $\text{B}-\text{H}^{\delta-}\cdots\delta^+\text{H}-\text{N}$ bonds,^{4,21} which may play a primary role in crystal packing and supramolecular assembly in molecular aggregations,²² although Merino argued that the aggregations

are mainly controlled by electrostatic dipole–dipole interactions instead of the dihydrogen interactions.²³

To gain insight into the electron transfer from the donor to the acceptor, it would be of particular importance if we can quantitatively express the ground and the first excited states in terms of the neutral (no-bond) and ionic (dative) resonance structures **1** and **2** and establish the novel structure–property relationships with the structural weight of the ionic structure **2**, as the extent to which electron transfer has occurred in donor–acceptor complexes can be measured by the ratio of the probabilities of dative and no-bond structures in the ground state, i.e., T_2/T_1 . It has been also presumed that due to the strong interaction between these two diabatic states, BH_3NH_3 is colorless.²⁴ Whereas it is difficult to derive a wave function for a resonance structure with the framework of MO theory, valence bond (VB) theory employs Heitler–London–Slater–Pauling (HLSP) function, which was proposed 60 years ago,^{18,19} to describe a resonance structure, and the molecular states are superimpositions of all possible HLSP functions.

Recently, we developed the block-localized wave function (BLW) method that incorporates the advantages of both VB and MO theories,^{25–27} i.e., the physical intuition of the VB theory and the computational efficiency of the MO theory. This BLW method provides the possibility to study various resonance structures (or diabatic states) at the cost of Hartree–Fock (HF) computations. On the basis of the BLW method, an energy decomposition scheme that can partition the intermolecular interaction energy into various energy terms such as electrostatic, exchange, polarization, and charge transfer has been proposed.^{10,28,29} This energy decomposition scheme is very similar to Stevens and Fink’s reduced variational space analysis.³⁰

In this work, we employed the modern ab initio VB method^{27,31,32} to study the EDA complex BH_3NH_3 and elucidate the nature of the electron-transfer interaction in terms of the two-state model.³³ We will use both the VB and BLW methods to explore the variation of electron transfer along the donor–acceptor distance. Similar to ethane, at the equilibrium geometry BH_3NH_3 prefers a staggered structure, and there is a substantial rotation barrier from the staggered to the eclipsed structure. Since controversies linger regarding the nature of the rotation barrier in ethane,³⁴ BH_3NH_3 is an excellent example to extend our exploration on the roles of the hyperconjugation and steric effects in the rotation barrier.

- (13) Mulliken, R. S.; Person, W. B. *Molecular Complexes*; Wiley: New York, 1969.
- (14) Gurjanova, E. N.; Goldstein, I. P.; Romm, I. P. *Donor–Acceptor Bond*; Wiley: New York, 1975.
- (15) Townes, C. H.; Dailey, B. P. *J. Chem. Phys.* **1949**, *17*, 782.
- (16) (a) Lucken, E. A. C. *Nuclear Quadrupole Coupling Constants*; Academic Press: London, 1969. (b) Gordy, W.; Cook, R. L. *Microwave Molecular Spectra*; Wiley: New York, 1984.
- (17) Thompson, W. H.; Hynes, J. T. *J. Am. Chem. Soc.* **2000**, *122*, 6278–6286.
- (18) Pauling, L. C. *The Nature of the Chemical Bond*, 3rd ed.; Cornell University Press: Ithaca, NY, 1960.
- (19) Wheland, G. W. *Resonance in Organic Chemistry*; Wiley: New York, 1955.
- (20) Haaland, A. *Angew. Chem., Int. Ed.* **1989**, *28*, 992–1007.
- (21) (a) Richardson, T.; de Gala, S.; Crabtree, R. H.; Siegbahn, P. E. M. *J. Am. Chem. Soc.* **1995**, *117*, 12875–12876. (b) Cramer, C. J.; Gladfelder, W. L. *Inorg. Chem.* **1997**, *36*, 5358–5362. (c) Custelcean, R.; Jackson, J. E. *Chem. Rev.* **2001**, *101*, 1963–1980.
- (22) Yokoyama, T.; Yokoyama, S.; Kamikado, T.; Okuno, Y.; Mashiko, S. *Nature* **2001**, *413*, 619–621.

- (23) Merino, G.; Bakhmutov, V. I.; Vela, A. J. *Phys. Chem. A* **2002**, *106*, 8491–8494.
- (24) Murrell, J. N.; Kettle, S. F. A.; Tedder, J. M. *The Chemical Bond*; Wiley: New York, 1978.
- (25) Mo, Y.; Peyerimhoff, S. D. *J. Chem. Phys.* **1998**, *109*, 1687–1697.
- (26) Mo, Y.; Zhang, Y.; Gao, J. *J. Am. Chem. Soc.* **1999**, *121*, 5737–5742.
- (27) Mo, Y.; Song, L.; Wu, W.; Cao, Z.; Zhang, Q. *J. Theor. Comput. Chem.* **2002**, *1*, 137.
- (28) Mo, Y.; Gao, J.; Peyerimhoff, S. D. *J. Chem. Phys.* **2000**, *112*, 5530–5538.
- (29) Mo, Y.; Subramanian, G.; Gao, J.; Ferguson, D. M. *J. Am. Chem. Soc.* **2002**, *124*, 4832–4837.
- (30) Stevens, W. J.; Fink, W. H. *Chem. Phys. Lett.* **1987**, *139*, 15–22.
- (31) (a) Wu, W.; Wu, A.; Mo, Y.; Zhang, Q. *Sci. China (Chinese Ed.)* **1995**, *B25*, 1247; (*English Ed.*) **1996**, *B39*, 456. (b) Wu, W.; Wu, A.; Mo, Y.; Lin, M.; Zhang, Q. *Int. J. Quantum Chem.* **1998**, *67*, 287–297. (c) Wu, W.; Mo, Y.; Cao, Z.; Zhang, Q. In *Valence Bond Theory*; Cooper, D. L., Ed.; Elsevier: Amsterdam, 2002; Vol. 10, p 143.
- (32) Wu, W.; Song, L.; Mo, Y.; Zhang, Q. XIAMEN99 – An ab initio valence bond (VB) program, Xiamen University, Xiamen, China, 2000.
- (33) Mo, Y.; Wu, W.; Zhang, Q. *J. Chem. Phys.* **2003**, *119*.
- (34) Mo, Y.; Wu, W.; Song, L.; Lin, M.; Zhang, Q.; Gao, J. *Angew. Chem., Int. Ed.*, in press.

Methodologies

Ab Initio VB Method. The most significant difference between the MO methods and VB methods is that in MO theory all orbitals are orthogonal, whereas in VB theory all orbitals are nonorthogonal. Often, the VB orbitals are restricted to a fraction of the whole space of basis functions. For example, they are often expanded in the basis functions of only one atom or a functional group. Since a molecule or reaction process can be described by a few resonance structures and each resonance structure is represented by a HLSP function, which is the linear combination of 2^m Slater determinants (m is the number of covalent bonds in the target system), the molecular states are expressed as linear combinations of VB functions.

For the case of BH_3NH_3 , the VB wave functions for the neutral (1) and ionic (2) resonance structures are defined as

$$\Phi_1 = N_1 \hat{A} [K_B K_N \sigma_{\text{BH}_1} \sigma_{\text{BH}_2} \sigma_{\text{BH}_3} \sigma_{\text{NH}_4} \sigma_{\text{NH}_5} \sigma_{\text{NH}_6} \sigma_{\text{NL}}] \quad (1)$$

$$\Phi_2 = N_2 \hat{A} [K_B K_N \sigma'_{\text{BH}_1} \sigma'_{\text{BH}_2} \sigma'_{\text{BH}_3} \sigma'_{\text{NH}_4} \sigma'_{\text{NH}_5} \sigma'_{\text{NH}_6} \sigma_{\text{NB}}] \quad (2)$$

where N_1 and N_2 are normalization factors, \hat{A} is an antisymmetrizer, and K_B and K_N are the core 1s orbitals for boron and nitrogen atoms, respectively. σ_{ij} in the above equations represents the following bond function:

$$\sigma_{ij} = \hat{A} \{ \phi_i(1) \phi_j(2) [\alpha(1)\beta(2) - \beta(1)\alpha(2)] \} \quad (3)$$

In the above equation, α and β are spin functions, and ϕ_i and ϕ_j are group orbitals that are expanded in either the BH_3 moiety ($X = \text{B}$) or the NH_3 moiety ($X = \text{N}$):

$$\phi_i = \sum_{k \in \text{XH}_3} c_{ik} \chi_k \quad (4)$$

The primes in eq 2 highlight that bond orbitals in eqs 1 and 2 are optimized simultaneously and are not necessary to be identical. In other words, different orbitals for different structures (or breathing orbitals^{35,36}) are adopted in this work. VBSCF computations with all possible resonance structures are comparable with the CASSCF method in the MO theory.³⁷ The fundamental difference between eqs 1 and 2 lies in the bond functions σ_{NL} and σ_{NB} . σ_{NL} denotes a nitrogen lone pair orbital, while σ_{NB} represents a central σ bond between boron and nitrogen.

Once we define the wave functions for the neutral and ionic resonance structures, the wave function for the EDA complex $\text{BH}_3\text{-NH}_3$ is expressed as

$$\Psi = C_1 \Phi_1 + C_2 \Phi_2 \quad (5)$$

and the structural weights of the neutral and ionic structure can be defined as

$$T_1 = C_1^2 + C_1 C_2 S_{12} \quad (6a)$$

$$T_2 = C_2^2 + C_1 C_2 S_{12} \quad (6b)$$

where S_{12} is the overlap integral between the two resonance structure wave functions.

On the basis of the above description, we can see that the ground state is computed with two resonance structures, and the computation may be termed as 2VBSCF since all coefficients are optimized self-consistently and simultaneously. The difficulty in the ab initio VB method lies in the evaluation of overlap and the Hamiltonian matrix elements among VB functions. During the past decade, the interests in

the development and applications of the modern ab initio VB methods grew with a few practical codes available.^{36,38} Work by numerous groups has demonstrated the capability of the VB methods to gain unique insights into chemical properties and reaction processes, albeit in small systems.^{37,39} Most recently, we developed a novel algorithm and implemented it into our code, Xiamen99, which makes the current computations feasible.^{27,31,32}

The adoption of group orbitals in this work excludes the introduction of the basis set superposition error (BSSE), which plagues the computation of intermolecular interactions, since no orbital is allowed to extend beyond one monomer. The energy difference between the 2VBSCF and the neutral resonance structure reflects the coupling between the neutral and ionic resonance structures and can be attributed to the electron-transfer stabilization energy

$$E_{\text{ct}}^{\text{VB}} = E(2\text{VBSCF}) - E(\Phi_1) \quad (7)$$

Since the bond orbitals in Φ_1 are localized on either the BH_3 or NH_3 monomer only, the relaxation of these bond orbitals wholly results from the external field imposed by the interacting partner. Thus, we can define the polarization energy as

$$E_{\text{pol}}^{\text{VB}} = E(\Phi_1^0) - E(\Phi_1) \quad (8)$$

where Φ_1^0 is constructed with the optimal orbitals in the monomers without further optimization.

Block-Localized Wave Function–Energy Decomposition (BLW–ED) Analysis. The BLW method is aimed to derive a resonance structure wave function which requires much less computational resources than the ab initio VB method.^{25,40} In the BLW method, all electrons and basis orbitals of a molecular system are partitioned into a few subgroups. Each molecular orbital in a subgroup is a linear combination of the primitive basis functions restricted in that particular subspace. This is in sharp contrast to the orbitals in MO methods that are expanded or delocalized over the whole system. As a consequence, in a BLW, which is constructed with a Slater determinant, orbitals in the same subgroups are constrained to be orthogonal, but those in the different subgroups are nonorthogonal.

For the case of BH_3NH_3 , the BLW corresponds to the neutral resonance structure **1** and is defined as

$$\Psi^{\text{BLW}} = \hat{A}(\Phi_{\text{BH}_3} \Phi_{\text{NH}_3}) \quad (9)$$

where Φ_{XH_3} is a successive product of the doubly occupied MOs in the XH_3 moiety ($X = \text{B}$ or N). Since orbitals in eq 9 are block-localized in either BH_3 or NH_3 and orbitals in the corresponding HF wave function Ψ^{HF} are extended in both BH_3 and NH_3 , the energy difference between Ψ^{BLW} and Ψ^{HF} after the basis set superposition error (BSSE) correction⁴¹ reflects the electron-transfer effect. In other words, the electron-transfer stabilization can be conveniently defined as

$$\Delta E_{\text{ct}} = E(\Psi^{\text{HF}}) - E(\Psi^{\text{BLW}}) + \text{BSSE} \quad (10)$$

The electron density difference between Ψ^{BLW} and Ψ^{HF} measures the magnitude of electron transfer from NH_3 to BH_3 .

(35) (a) Hiberty, P. C.; Humbel, S.; Byrman, C. P.; van Lenthe, J. H. *J. Chem. Phys.* **1994**, *101*, 5969–5976. (b) Hiberty, P. C.; Shaik, S. *Theor. Chem. Acc.* **2002**, *108*, 255–272.

(36) Hiberty, P. C. *THEOCHEM* **1997**, 398–399, 35–43.

(37) Raimondi, M.; Cooper, D. L. *Top. Curr. Chem.* **1999**, *203*, 105–120.

(38) (a) *Valence Bond Theory*; Cooper, D. L., Ed.; Elsevier: Amsterdam, 2002. (b) Cooper, D. L.; Gerratt, J.; Raimondi, M. *Nature* **1986**, *323*, 699. (c) Cooper, D. L.; Gerratt, J.; Raimondi, M. *Chem. Rev.* **1991**, *91*, 929. (d) McWeeny, R. *Int. J. Quantum Chem.* **1999**, *74*, 87–96. (e) McWeeny, R. *Int. J. Quantum Chem.* **1988**, *34*, 25. (f) Gallup, G. A.; Vance, R. L.; Collins, J. R.; Norbeck, J. M. *Adv. Quantum Chem.* **1982**, *16*, 229–272. (g) Dijkstra, F.; van Lenthe, J. H. *J. Chem. Phys.* **2000**, *113*, 2100–2108.

(39) (a) Hiberty, P. C.; Byrman, C. P. *J. Am. Chem. Soc.* **1995**, *117*, 9870–9880. (b) Lauvergnat, D.; Maitre, P.; Hiberty, P. C.; Volatron, F. *J. Phys. Chem.* **1996**, *100*, 6463–6468. (c) Shaik, S.; Shurki, A. *Angew. Chem., Int. Ed.* **1999**, *38*, 586–625. (d) Mo, Y.; Wu, W.; Zhang, Q. *J. Phys. Chem.* **1994**, *98*, 10048–10053. (e) Mo, Y.; Lin, Z.; Wu, W.; Zhang, Q. *J. Phys. Chem.* **1996**, *100*, 6469–6474.

(40) Mo, Y. *J. Chem. Phys.* **2003**, *119*, 1300–1306.

(41) Boys, S. F.; Bernardi, F. *Mol. Phys.* **1970**, *19*, 553–566.

Similar to the VB treatment, we can examine the polarization effect using the wave functions of monomers ($\Phi_{\text{BH}_3}^0$ and $\Phi_{\text{NH}_3}^0$) by defining a zero-order BLW as

$$\Psi^{\text{BLW}0} = \hat{A}(\Phi_{\text{BH}_3}^0 \Phi_{\text{NH}_3}^0) \quad (11)$$

Subsequently, the polarization energy is defined as

$$\Delta E_{\text{pol}} = E(\Psi^{\text{BLW}0}) - E(\Psi^{\text{BLW}}) \quad (12)$$

In fact, on the basis of the BLW–ED, the HF intermolecular interaction between BH_3 and NH_3 can be broken down into geometry distortion (ΔE_{dist}), electrostatic (ΔE_{es}), exchange repulsion (ΔE_{ex}), polarization (ΔE_{pol}), and charge-transfer (ΔE_{ct}) energy terms:

$$\Delta E_{\text{HF}} = \Delta E_{\text{dist}} + \Delta E_{\text{es}} + \Delta E_{\text{ex}} + \Delta E_{\text{pol}} + \Delta E_{\text{ct}} \quad (13)$$

where ΔE_{dist} is the distortion energy of the monomers, corresponding to the change from the equilibrium geometries of isolated monomers to those in the EDA complex. The electrostatic energy is evaluated by defining a Hartree product of the two monomer Slater determinants

$$\Psi^{\text{H}} = \Phi_{\text{BH}_3}^0 \Phi_{\text{NH}_3}^0$$

and

$$\Delta E_{\text{es}} = E(\Psi^{\text{H}}) - E(\Phi_{\text{BH}_3}^0) - E(\Phi_{\text{NH}_3}^0) \quad (14)$$

The exchange repulsion energy originates from the antisymmetry of electrons between two monomers:

$$\Delta E_{\text{ex}} = E(\Psi^{\text{BLW}0}) - E(\Psi^{\text{H}}) \quad (15)$$

The definition of the electrostatic and exchange energy terms are identical to the Morokuma decomposition scheme.⁴² In comparison with the Morokuma scheme, the BLW decomposition method exhibits much less dependency on the basis set used in the calculation. With the introduction of an additional electron correlation energy contribution term, ΔE_{corr} , the BLW–ED analysis can be further extended to higher levels. For example, at the MP2 level, the intermolecular interaction between two monomers is

$$\Delta E_{\text{MP}2} = \Delta E_{\text{dist}} + \Delta E_{\text{es}} + \Delta E_{\text{ex}} + \Delta E_{\text{pol}} + \Delta E_{\text{ct}} + \Delta E_{\text{corr}} \quad (16)$$

where the terms ΔE_{es} , ΔE_{ex} , ΔE_{pol} , and ΔE_{ct} are identical to those in eq 13, but ΔE_{dist} is the energy required to distort the monomers at the MP2 level, and ΔE_{corr} reflects the difference between the vertical interaction energies computed at the MP2 and HF levels.

Computational Details

Most computational studies on electron donor–acceptor complexes have focused on the equilibrium geometries of electron donor–acceptor complexes, and the effects of computation levels have been well understood. Horváth et al.¹¹ demonstrated that the MP2(fc)/6-311+G(2df,p) level is sufficient to study the electron-transfer effect in a wide range between 1.5 and 10 Å of the donor–acceptor distance. Since the ab initio VB method is comparable with the CASSCF method and computationally demanding, we employed the 6-31G(d) basis set to run VB computations. To derive the energy profiles of both neutral and ionic states (eqs 1 and 2) for BH_3NH_3 , we first optimized the geometry of the complex with constrained $r(\text{B}-\text{N})$ distance at the MP2/6-31G(d) level, followed by two 1VBSCF computations. The energy profile for the ground state of BH_3NH_3 was subsequently computed at

(42) Kitaura, K.; Morokuma, K. *Int. J. Quantum Chem.* **1976**, *10*, 325–340.

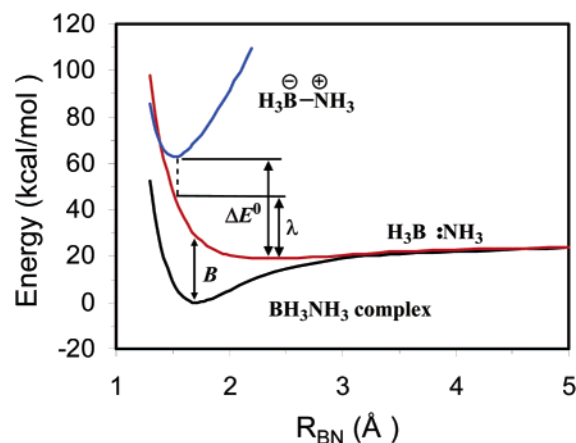


Figure 1. Ab initio VB energy profiles for the diabatic states (blue and red lines) and adiabatic state (black line) with the 6-31G(d) basis set.

the 2VBSCF/6-31G(d)//MP2/6-31G(d) level. In all VB calculations, group localized orbitals were adopted to distinguish the two resonance structures.

Similarly, the BLW–ED analysis was conducted at the MP2/6-31G(d) geometries. To examine the basis set dependency, however, we also performed MP2/6-311+G(d,p) optimizations followed by the BLW–ED analysis. Since the BLW corresponds to the diabatic state where the electron transfer between BH_3 and NH_3 is prohibited, the population analysis on the BLW as well as the HF wave function elucidated the amount of electron transferred from the donor to the acceptor. Various population analyses, including the Mulliken analysis, natural population analysis (NPA),⁴³ and dipole-moment-based analysis were employed to estimate the amount of electron transferred from the donor NH_3 to the acceptor BH_3 .

Throughout the work, geometry optimizations and the calculations of the primitive integrals that were required for VB and BLW calculations were performed with the Gaussian98 software,⁴⁴ while VB and BLW calculations were performed with in-house codes.^{32,45}

Results and Discussion

Two-State Model for BH_3NH_3 . Energy profiles for the neutral state **1** and ionic state **2** together with the ground state were derived at the VBSCF/6-31G(d)//MP2/6-31G(d) level and shown in Figure 1. The energy curve for the ground state is very similar to those obtained with MO methods,¹¹ although the equilibrium N–B distance (~ 1.70 Å) is slightly longer than high-level MO theoretical level computations (1.664 and 1.656 Å at the MP2/6-31G(d) and MP2/6-311+G(d,p) levels, respectively) and experimental data (1.6576 Å³), and the binding energy between NH_3 and BH_3 (-23.9 kcal/mol) is somewhat underestimated compared with the value at the MP2 level with 6-31G(d) (-28.2 kcal/mol) or 6-311+G(d,p) (-27.5 kcal/mol)

(43) (a) Foster, J. P.; Weinhold, F. *J. Am. Chem. Soc.* **1980**, *102*, 7211–7218. (b) Reed, A. E.; Curtiss, L. A.; Weinhold, F. *Chem. Rev.* **1988**, *88*, 899–926.

(44) Frisch, M. J.; Trucks, G. W.; Schlegel, H. B.; Scuseria, G. E.; Robb, M. A.; Cheeseman, J. R.; Zakrzewski, V. G.; Montgomery, J. A., Jr.; Stratmann, R. E.; Burant, J. C.; Dapprich, S.; Millam, J. M.; Daniels, A. D.; Kudin, K. N.; Strain, M. C.; Farkas, O.; Tomasi, J.; Barone, V.; Cossi, M.; Cammi, R.; Mennucci, B.; Pomelli, C.; Adamo, C.; Clifford, S.; Ochterski, J.; Petersson, G. A.; Ayala, P. Y.; Cui, Q.; Morokuma, K.; Malick, D. K.; Rabuck, A. D.; Raghavachari, K.; Foresman, J. B.; Cioslowski, J.; Ortiz, J. V.; Stefanov, B. B.; Liu, G.; Liashenko, A.; Piskorz, P.; Komaromi, I.; Gomperts, R.; Martin, R. L.; Fox, D. J.; Keith, T.; Al-Laham, M. A.; Peng, C. Y.; Nanayakkara, A.; Gonzalez, C.; Challacombe, M.; Gill, P. M. W.; Johnson, B. G.; Chen, W.; Wong, M. W.; Andres, J. L.; Head-Gordon, M.; Replogle, E. S.; Pople, J. A. *Gaussian 98*, revision A.9; Gaussian, Inc.: Pittsburgh, PA, 1998.

(45) Mo, Y.; Gao, J. *Block-Localized Wave Function (BLW)*, version 1.0; University of Minnesota: Minneapolis, MN, 2000.

as well as at the QCISD/aug-cc-pVTZ level (-29.4 kcal/mol¹¹). However, it should be noted that the latter optimizations are conducted for the dimer with the contamination of the BSSE effect. The interesting features with the modern ab initio VB calculations are the energy curves for the diabatic states which are unavailable from MO theory-based methods. For the neutral resonance state **1**, the energy curve purely reflects the nonbonded interactions which include the conventional van der Waals (mainly the electrostatic and exchange) interactions, because there is no electron penetration between the two monomers. The shallow and flat minimum area corresponds to the weak attraction between NH_3 and BH_3 , which can be well fitted by many potential functions such as the Lennard-Jones form. We found that the minimum is -5.2 kcal/mol at the separation $R_{\text{BN}} = 2.33$ Å. For comparison, the covalent radii for nitrogen and boron are 0.75 and 0.82 Å, respectively, and the van der Waals radius for nitrogen is 1.55 Å, but it is not available for boron due to the lack of experimental data.⁴⁶ However, it is certain that the equilibrium distance in the neutral resonance structure (2.33 Å) must be shorter than the sum of van der Waals radii for nitrogen and boron due to the electrostatic interactions, because nitrogen is an electronegative atom and boron is an electropositive atom, as compared with hydrogen atoms.

The energy curve for the ionic resonance structure is of a deep well which is the characteristic for electrostatic interactions, and the minimum locates at $R_{\text{BN}} = 1.51$ Å. The two diabatic potential energy surfaces cross at $R_{\text{BN}} = 1.39$ Å, and their relative position indicates that the electron transfer from NH_3 to BH_3 falls in the inverted or abnormal region as the reorganization energy λ is smaller than the exoergicity $|\Delta E^\circ|$,^{47,48} as illustrated in Figure 1. In the polar media, the ionic structure will be much more significantly stabilized than the neutral structure and its energy surface will shift downward, and eventually the electron transfer from NH_3 to BH_3 may fall in the normal region ($\lambda > |\Delta E^\circ|$).

The most surprising feature in Figure 1 perhaps is the strong coupling between the neutral state and the ionic state in the binding region, even when their energy difference is very substantial. For instance, at the equilibrium geometry of the complex, the energy difference between the two diabatic states is 40.0 kcal/mol, but the coupling energy B between the two states relative to the more stable neutral state amounts to 29.1 kcal/mol. As a consequence, the current electron-transfer process can be classified as being “adiabatic”.⁴⁸

Figure 2 plots the structural weights of the two diabatic state with respect to the distance between NH_3 and BH_3 . With the approaching of the donor and acceptor, the structural weight of the neutral resonance structure decreases dramatically, whereas that of the ionic state increases reversely. This figure highlights the occurrence of the charge transfer from the donor to the acceptor.

Energetic Analysis and Electron-Transfer Effect. We have examined the interactions in many donor–acceptor complexes including BH_3NH_3 with various basis sets at their equilibrium

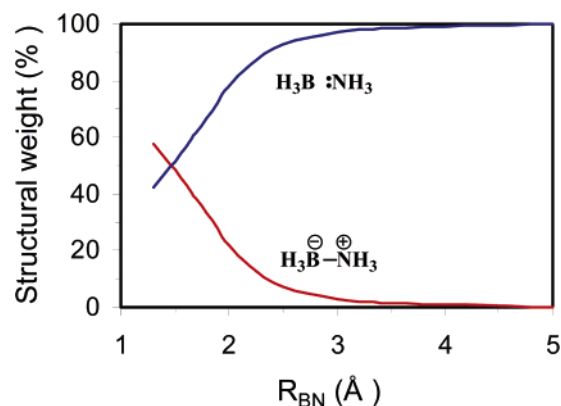


Figure 2. Structural weights of the diabatic states along the donor–acceptor distance based on the VBSCF/6-31G(d) computations.

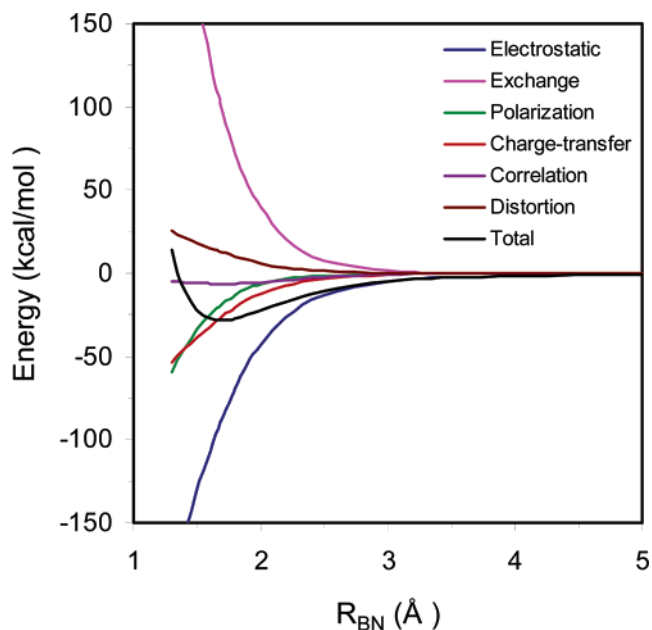


Figure 3. Variation of various energy terms with respect to the donor–acceptor distance computed with the 6-31G(d) basis set.

geometries.^{10,28,49} Although we have demonstrated that the BLW–ED analysis is much more stable than Morokuma’s⁴² with the variation of basis sets, studies on the case of BH_3NH_3 with 6-31G(d), 6-311+G(d,p), and cc-pVTZ basis sets revealed a moderate increasing of the polarization energy with the enlargement of the basis set while the sum of the electrostatic and Pauli exchange energies decreases at the same magnitude. In other words, the charge-transfer energy term is essentially independent of the basis sets. To examine the dependence of individual energy terms on the donor–acceptor distance, we explore here the detailed energy profiles with respect to the separation between NH_3 and BH_3 at the MP2 level with 6-31G(d) and 6-311+G(d,p), as shown in Figures 3 and 4, respectively. Virtually, both figures are very similar, suggesting the basis set dependency is very modest and at least will not affect our discussions and conclusions in a noticeable way. Clearly, the electrostatic attraction is a long-range interaction, while the Pauli exchange repulsion starts to play a role in the van der Waals regime (~ 3 Å). Thus, in accord with conventional theories, the

(46) Bondi, A. J. *Phys. Chem.* **1964**, *68*, 441–451.

(47) (a) Marcus, R. A. *J. Chem. Phys.* **1956**, *24*, 966–978. (b) Marcus, R. A. *J. Chem. Phys.* **1956**, *24*, 979–989. (c) Marcus, R. A. *J. Chem. Phys.* **1965**, *43*, 679–701. (d) Marcus, R. A.; Sutin, N. *Biochim. Biophys. Acta* **1985**, *811*, 265–322. (e) Newton, M. D.; Sutin, N. *Annu. Rev. Phys. Chem.* **1984**, *35*, 437–480. (f) Farazdel, A.; Dupuis, M.; Clementi, E.; Aviram, A. *J. Am. Chem. Soc.* **1990**, *112*, 4206–4214.

(48) Mikkelsen, K. V.; Ratner, M. A. *Chem. Rev.* **1987**, *87*, 113–153.

(49) Fiacco, D. L.; Mo, Y.; Hunt, S. W.; Ott, M. E.; Roberts, A.; Leopold, K. R. *J. Phys. Chem. A* **2001**, *105*, 484–493.

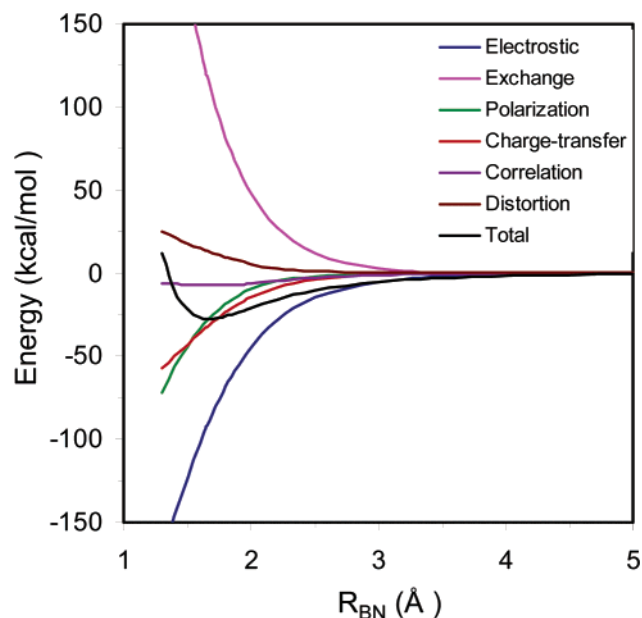


Figure 4. Variation of various energy terms with respect to the donor–acceptor distance computed with the 6-311+G(d,p) basis set.

van der Waals interaction can be well described by the balance between the electrostatic attraction and the Pauli exchange repulsion, which varies exponentially with the approach of the donor and acceptor. However, the Pauli exchange repulsion increases with the shortening of the donor–acceptor distance at a magnitude much larger than the electrostatic stabilization and dominates the overall interaction between NH_3 and BH_3 rapidly when the distance is shorter than 1.5 Å.

Interestingly, both the polarization energy and charge-transfer stabilization energy increase absolutely in an exponential pattern, although both are important only at short distances. In the binding regime ($R_{\text{BN}} > 1.5$ Å), the charge-transfer effect is more important than the polarization. As a matter of fact, at the equilibrium, the magnitude of the charge-transfer stabilization is the same as the overall interaction energy.

With the deactivation of the electron transfer between NH_3 and BH_3 , the geometrical optimization with the BLW method⁴⁰ can result in a complex where the van der Waals interaction rules. It is worthwhile to note that the BLW optimization in the current case is identical to the SCF-MI (self-consistent field for molecular interaction) method which was developed by Gianinetti, Raimondi, and their co-workers⁵⁰ and implemented into the GAMESS-US software,⁵¹ although the SCF-MI was proposed to find a BSSE-free solution and the charge-transfer energy term defined in the present BLW–ED approach as eq 10 would be completely assigned to the BSSE contribution. In our opinion, the SCF-MI or BLW method provides an ideal approach to estimate the van der Waals interactions among systems where the electron transfers are screened out. We conducted BLW optimizations on BH_3NH_3 and compared the optimal geometries with those derived at the MP2 and HF levels where the charge transfer is permitted. Results are compiled in

Table 1. Equilibrium Geometries of BH_3NH_3 at Various Theoretical Levels^a

	R_{BN}	R_{BH}	R_{NH}	$\angle\text{HBN}$	$\angle\text{HNB}$
MP2/6-31G(d)	1.664	1.210	1.020	104.5	111.1
MP2/6-311+G(d,p)	1.656	1.208	1.017	104.7	111.2
HF/6-31G(d)	1.689	1.209	1.004	104.3	110.9
HF/6-311+G(d,p)	1.680	1.210	1.003	104.6	110.8
BLW/6-31G(d)	2.295	1.191	1.003	95.4	111.7
BLW/6-311+G(d,p)	2.607	1.190	1.001	93.3	111.1

^a Bond distances are given in angstroms, bond angles are given in degrees.

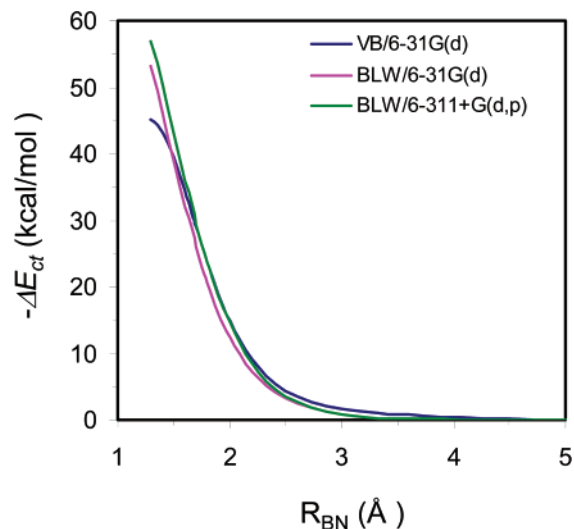


Figure 5. Comparison of the charge-transfer stabilization energies along the donor–acceptor distance derived from the ab initio VB and BLW approaches.

Table 1. Whereas we found that the N–B distance in the BLW optimizations is much longer than the MP2 or HF results, the large fluctuation with the basis sets reinforces our discussion in the last section about the flatness of the van der Waals energy surface in the bottom area. The van der Waals distances between NH_3 and BH_3 are 2.295 and 2.607 Å with the 6-31G(d) and 6-311+G(d,p) basis sets, respectively, in accord with 2.33 Å from the ab initio VB method and 6-31G(d) basis set (Figure 1). Compared with the stable monomers, the computed van der Waals energy is 5.80 or 3.74 kcal/mol with the 6-31G(d) and 6-311+G(d,p) basis set. If we do not account for the distortion energies consumed in the formation of van der Waals complex of BH_3NH_3 , the vertical van der Waals energy is 7.71 or 4.45 kcal/mol with the 6-31G(d) and 6-311+G(d,p) basis set.

Because our main interest in this work is the charge transfer in the electron donor–acceptor complex BH_3NH_3 , we compared the charge-transfer stabilization obtained with the ab initio VB and BLW methods in Figure 5. Obviously, the energy profiles are almost identical. This indicates that our approach to derive the charge-transfer energy is independent of both the methods and basis sets. The artifact of the basis set will be reflected primarily in other energy terms such as the polarization, electrostatic, and Pauli exchange energies.

A more interesting, yet less physical issue, is the estimation of the amount of charge transferred from the donor to the acceptor. Although the concept of partial charge in molecules is nonphysical and the computational determination is very much dependent on the methods, often it is intuitive to derive the partial charges in order to generate a physical picture illustrating

(50) (a) Gianinetti, E.; Raimondi, E. *Int. J. Quantum Chem.* **1996**, *60*, 157–166. (b) Famulari, A.; Gianinetti, E.; Raimondi, M.; Sironi, M. *Int. J. Quantum Chem.* **1998**, *69*, 151–158.

(51) Schmidt, M. W.; Baldrige, K. K.; Boatz, J. A.; Elbert, S. T.; Gordon, M. S.; Jensen, J. J.; Koseki, S.; Matsunaga, N.; Nguyen, K. A.; Su, S.; Windus, T. L.; Dupuis, M.; Montgomery, J. A. *J. Comput. Chem.* **1993**, *14*, 1347–1363.

the flowing of electrons apart from the immediate utilization in molecular mechanics. Numerous procedures to perform population (or charge) analysis have been proposed and extensively reviewed.⁵² Here we adopt the popular Mulliken analysis (MA) and the natural population analysis (NPA) to generate the partial charges for atoms. The NPA is known to be insensitive to the basis set. Since the intermediate wave function Ψ^{BLW} defined as eq 9 corresponds to the state where the electron transfer between NH_3 and BH_3 is deactivated, the population analysis should find a net zero flow of electrons from NH_3 to BH_3 . This is indeed the case in the Mulliken analysis, where the overlap integrals are equally partitioned to the pairing atoms. However, in most other procedures such as the NPA, the analysis is conducted on the overall electron density of the complex, and a nonzero flow of electrons will be found in Ψ^{BLW} . While this origin requires further investigation, for the time being we simply take this amount as the residual charge transfer and deduct it from the value in the delocalized wave function Ψ^{HF} .¹⁰ In other words, we defined the amount of electron transferred as

$$\Delta q = q_{\text{BH}_3}(\Psi^{\text{HF}}) - q_{\text{BH}_3}(\Psi^{\text{BLW}}) = q_{\text{NH}_3}(\Psi^{\text{BLW}}) - q_{\text{NH}_3}(\Psi^{\text{HF}}) \quad (17)$$

where q_{BH_3} or q_{NH_3} is the population derived from the wave function Ψ^{BLW} or Ψ^{HF} . Experimentally, the charge-transfer effect is estimated on the basis of the nuclear hyperfine parameters.^{3,16} However, we have found that the polarization of the monomers (especially the Lewis acids) and the charge-transfer effects contribute almost equally to the variation of dipole moment in a Lewis acid–base adduct compared with the sum of dipole moments of separated monomers.^{10,49} As a result, the experimental estimation may significantly overestimate the degree of charge transfer. On the basis of the dipole moment data, we propose a dipole moment-based analysis (MDA) to measure the magnitude of charge transferred:

$$\Delta q = \frac{\mu^{\text{HF}} - \mu^{\text{BLW}}}{R_{\text{BN}}} \quad (18)$$

where μ^{HF} and μ^{BLW} are the dipole moments for Ψ^{HF} and Ψ^{BLW} , respectively. Figure 6 plotted the charge-transfer effect with respect to the donor–acceptor distance with the three procedures and two basis sets. Compared with the MA and MDA, the NPA shows negligible basis set dependency. Remarkably, however, we found a significant dependency of the estimation of the charge transfer on the population analysis schemes. Whereas the Mulliken scheme shows a monotonic increase of the magnitude of charge transfer with the shortening of the NH_3 and BH_3 distance, both the natural population and dipole moment-based schemes reveal a maxima of the amount of electron transferred in the range of 1.7 to 1.8 Å. A rational estimation of the amount of electron transferred may be based on the electron density difference between Ψ^{HF} and Ψ^{BLW} . The comparison between Figures 5 and 6 suggests that the study of the electron-transfer effect may focus on the energetics, which show much less dependency on both the method and basis set, rather than the evaluation of the amount of electrons transferred,

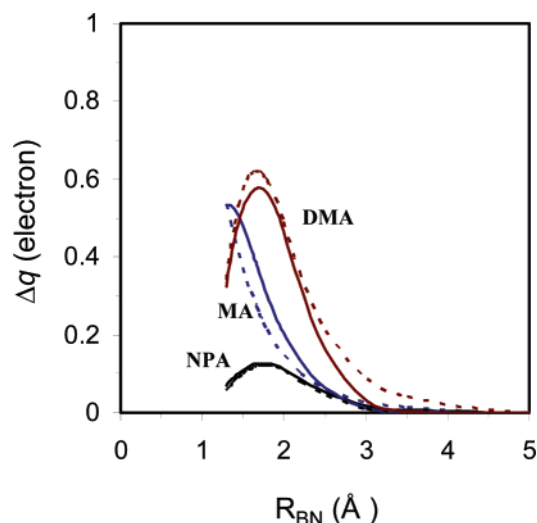


Figure 6. Estimation of the amount of electron transferred from NH_3 to BH_3 with various schemes (NPA: natural population analysis; MA: Mulliken analysis; DMA: dipole moment analysis) and basis sets (solid line: 6-311+G(d,p); dashed line: 6-31G(d)).

although it is still very insightful to conduct such an analysis for a series of donor–acceptor systems with the same method and basis set.^{10,49}

Nature of the Rotation Barrier in BH_3NH_3 . Recently, there has been a resurging interest in the nature of rotation barriers in small molecules such as ethane, initiated by a series works by Goodman and co-workers.⁵³ Conventionally, it is believed that the Pauli repulsion between the two methyl groups leads to the stabilization of the staggered conformer.^{18,54} Later, a hyperconjugation model was proposed to explain the rotational barrier of around 3 kcal/mol in ethane.⁵⁵ In the hyperconjugation model, it is demonstrated that interaction between σ_{CH} occupied orbitals in one methyl group and σ_{CH}^* antibonding orbitals in the other methyl group dominantly favors the staggered conformer. Goodman's group furthered the hyperconjugation theory and claimed that the eclipsed structure would be preferred if hyperconjugation interactions were screened out. Apart from the main competing steric repulsion and hyperconjugation models,⁵⁶ there are other explanations for the origin of the ethane rotation barrier.⁵⁷ Importantly, we note that the hyperconjugation explanation is put forward based on post-SCF analyses where the lack of relaxation for the localized bond orbitals may notably overestimate the hyperconjugative stabilization.²⁵ Our most recent study with both BLW and ab initio VB methods, which are able to self-consistently derive the localized orbitals and wave functions, concluded that the hyperconjugative interaction

(52) (a) Wiberg, K. B.; Rablen, P. R. *J. Comput. Chem.* **1993**, *14*, 1504–1518. (b) Sigfridsson, E.; Ryde, U. *J. Comput. Chem.* **1998**, *19*, 377–395.

(53) (a) Goodman, L.; Gu, H. *J. Chem. Phys.* **1998**, *109*, 72–78. (b) Goodman, L.; Gu, H.; Pophristic, V. *J. Chem. Phys.* **1999**, *110*, 4268–4275. (c) Goodman, L.; Pophristic, V.; Weinhold, F. *Acc. Chem. Res.* **1999**, *32*, 983–993. (d) Pophristic, V.; Goodman, L. *Nature* **2001**, *411*, 565–568. (54) Sovers, O. J.; Kern, C. W.; Pitzer, R. M.; Karplus, M. *J. Chem. Phys.* **1968**, *49*, 2592–2599. (55) (a) Brunck, T. K.; Weinhold, F. *J. Am. Chem. Soc.* **1979**, *101*, 1700–1709. (b) Reed, A. E.; Weinhold, F. *Isr. J. Chem.* **1991**, *31*, 277–285. (56) (a) Houk, K. N.; Rondan, N. G.; Brown, F. K. *Isr. J. Chem.* **1983**, *23*, 3–9. (b) Houk, K. N.; Rondan, N. G.; Brown, F. K.; Jorgensen, W. L.; Madura, J. D.; Spellmeyer, D. C. *J. Am. Chem. Soc.* **1983**, *105*, 5980–5988. (c) Bickelhaupt, F. M.; Baerends, E. J. *Angew. Chem., Int. Ed.* **2003**, *42*, 4183–4188. (d) Weinhold, F. *Angew. Chem., Int. Ed.* **2003**, *42*, 4188–4194. (57) (a) Allen, L. C. *Chem. Phys. Lett.* **1968**, *2*, 597. (b) Payne, P. W.; Allen, L. C. In *Modern Theoretical Chemistry*; Schaefer, H. F., III, Ed.; Plenum Press: New York and London, 1977; Vol. 4, pp 29–108. (c) Bader, R. F. W.; Cheeseman, J. R.; Laidig, K. E.; Wiberg, K. B.; Breneman, C. J. *Am. Chem. Soc.* **1990**, *112*, 6530–6536.

Table 2. Energy Variations between the Staggered and Eclipsed Conformers of BH_3NH_3 Based on the BLW Energy Decomposition Analysis (kcal/mol)

basis set	structure	ΔE_{es}	ΔE_{ex}	ΔE_{pol}	ΔE_{ct}	ΔE_{tot}
6-31G(d)	staggered	-93.5	106.9	-20.5	-28.0	-35.1
	eclipsed	-94.0	109.3	-20.6	-27.4	-32.6
	$\Delta\Delta E$	-0.4	2.4	-0.2	0.7	2.5
6-311+G(d,p)	staggered	-91.9	119.0	-28.6	-32.1	-33.6
	eclipsed	-92.3	121.5	-28.8	-31.5	-31.1
	$\Delta\Delta E$	-0.4	2.5	-0.2	0.7	2.6

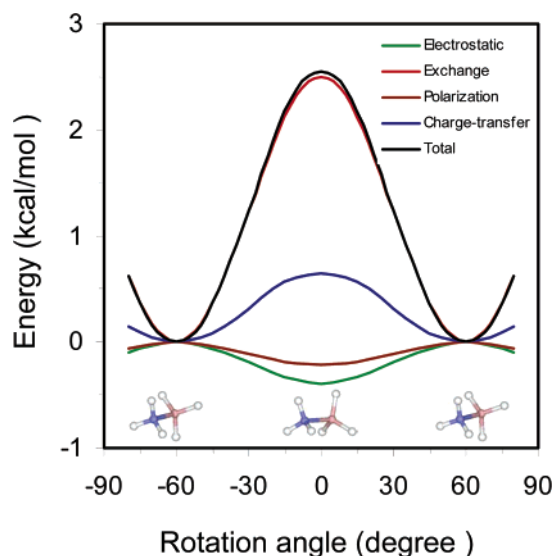
between the two methyl groups in ethane accounts for only one-third of the total torsional barrier in ethane, and the steric repulsion dominates the preference of the staggered conformer over the eclipsed conformer.³⁴

As an isoelectronic system with ethane, BH_3NH_3 provides an ideal example to examine our findings in the case of ethane. The advantage in the case of BH_3NH_3 is that two moieties can be completely separated in the intermediate BLW, whereas in ethane the covalent bond between two carbon atoms limits the application of the BLW method. The disadvantage in the study of the rotation barrier in BH_3NH_3 is that the hyperconjugative interactions between σ_{NH} and σ_{BH}^* and between σ_{BH} and σ_{NH}^* are included in the large charge-transfer energy term which is overwhelmed by the $\text{N} \rightarrow \text{B}$ dative bond energy, which would be very sensitive to the bond lengths. Consequently, the fluctuation of the dative bond strength may significantly perturb the estimation of the hyperconjugative stabilization. To minimize the fluctuation, we start from the optimal staggered geometry at the MP2 level and keep all structural parameters unchanged except the rotation angle around B–N bond. In this way, we can be certain that the $\text{N} \rightarrow \text{B}$ σ bond is conserved in the rotation process. The subsequent BLW energy analyses on the staggered and eclipsed conformers of BH_3NH_3 with both the 6-31G(d) and 6-311+G(d,p) basis sets generate the energy variations from electrostatic, exchange, polarization, and charge transfer, which are compiled in Table 2.

Although individual energy terms slightly fluctuate with the basis set, the differences of all energy terms between the staggered and eclipsed conformers show negligible basis set dependency. This allows us to reliably survey the nature of the rotation barrier. Similar to the case of ethane, we found that the charge-transfer effect prefers the staggered structure. If the $\text{N} \rightarrow \text{B}$ σ bond is truly conserved, the charge-transfer energy change comes from the hyperconjugation effect between NH_3 and BH_3 . Both the electrostatic and polarization interactions slightly favor the eclipsed structure, in accord with the different natures of the hydrogen atoms in the two moieties.^{4,21} Figure 7 further shows the details of all energy variations in the process of rotation. Evidently, both Table 2 and Figure 7 reveal that the Pauli exchange repulsion dominates the rotation barrier in BH_3NH_3 and that its magnitude is interestingly the same as the overall barrier. If we sum the electrostatic, exchange, and polarization terms as the steric effect, we can reasonably conclude that the steric effect plays the driving force in the rotation barrier around the B–N bond and the hyperconjugative interaction plays a secondary role. In other words, the nature of the rotation barrier in BH_3NH_3 is the same as that in ethane.³⁴

Conclusions

Because the VB theory is superior to the MO theory in the aspect that the former can distinctively define the individual

**Figure 7.** Relative energy variations around the rigid rotation at the HF/6-311+G(d,p) level.

diabatic states (resonance structures), modern ab initio VB computations can be used to study the two-state model, which has been proposed for the electron donor–acceptor (EDA) complexes, at the quantitative level. We employed the VB method to plot the energy surfaces of the two diabatic states, including one neutral no-bond state and one ionic electron-transferred state, for the typical EDA complex BH_3NH_3 . The relative positions of these two diabatic state energy profiles manifest that the electron transfer between NH_3 and BH_3 belongs to the abnormal region in electron transfer theory since the reorganization energy is even less than the reaction energy. Although at the equilibrium geometry of the complex the ionic state is much less stable than the neutral state, the coupling between them is very strong. In fact, this has been anticipated to explain the colorlessness of the compound.²⁴ For example, at the B–N distance of 1.66 Å, the energy difference between the two diabatic states is 35.8 kcal/mol, but the coupling energy between the two states relative to the more stable neutral state reaches 31.0 kcal/mol, and the structural weights of the neutral and ionic states are 59.4 and 40.6%, respectively.

The nature of the donor–acceptor interaction can be well probed by our developed BLW energy analysis. Interestingly, we found that the charge-transfer stabilization versus the donor–acceptor distance is essentially invariant for either VB or BLW method with either 6-31G(d) or 6-311+G(d,p) basis set. However, the estimation of the electron transferred from NH_3 to BH_3 is less successful since it heavily depends on the population analysis procedures. A promising approach may be the population analysis on the electron density difference between the HF and BLW wave functions, rather than on the HF and BLW electron densities followed by a deduction.

Our approach can further be applied to the exploration of the nature of the rotation barrier in BH_3NH_3 , which is isoelectronic with ethane. Although conventionally the preference of the staggered conformer over the eclipsed conformer of ethane was attributed to the repulsion between the two adjacent methyl groups, recent studies claimed the hyperconjugation effect between the two groups is the origin of the rotation barrier. Since the interaction between two monomers can be probed in detail with the BLW method, we feel that the BLW analysis

on the staggered and eclipsed structures of BH_3NH_3 can shed light on the controversy over the nature of rotation barriers. With rigid rotations, we calibrated the changes of all energy terms along the way and found that although the charge-transfer effect where the hyperconjugation effect is included indeed favors the staggered structure, the Pauli repulsion dominates the rotation and is essentially responsible for the preference of the staggered structure, while both the electrostatic and polariza-

tion slightly favor the eclipsed structure. This conclusion is in accord with our recent studies on ethane.

Acknowledgment. This work has been supported by the Western Michigan University (Y.M.). We are grateful to the generous support from the National Natural Science Foundation of China (Nos. 20225311 and 20021002).

JA039778L